Quantum spin circulator in Y junctions of Heisenberg chains

Quantum spin circulator in Y junctions of Heisenberg chains

Francesco Buccheri,[1] Reinhold Egger,[1] Rodrigo G. Pereira,[2] and Flávia B. Ramos[2]

[1] *Institut für Theoretische Physik, Heinrich-Heine-Universität, D-40225 Düsseldorf, Germany*

[2] *International Institute of Physics, Universidade Federal do Rio Grande do Norte, Campus Universitario, Lagoa Nova, Natal-RN 59078-970, Brazil*

(Received 14 January 2018; published 11 June 2018)

We show that a quantum spin circulator, a nonreciprocal device that routes spin currents without any charge transport, can be achieved in Y junctions of identical spin-1/2 Heisenberg chains coupled by a chiral three-spin interaction. Using bosonization, boundary conformal field theory, and density matrix renormalization group simulations, we find that a chiral fixed point with maximally asymmetric spin conductance arises at a critical point separating a regime of disconnected chains from a spin-only version of the three-channel Kondo effect. We argue that networks of spin-chain Y junctions provide a controllable approach to construct long-sought chiral spin-liquid phases.

DOI: 10.1103/PhysRevB.97.220402

Introduction. The spin-1/2 Heisenberg chain represents an analytically accessible model of basic importance in condensed matter theory [1]. By now, many experimental and theoretical works have contributed to a rather complete understanding of this model, including the effects of boundaries and junctions of two chains [2]. However, little attention has been devoted to quantum junctions formed by more than two Heisenberg chains. In fact, recent theoretical developments provide hints that interesting physics should be expected in that direction: First, multichannel Kondo fixed points have been predicted for junctions of anisotropic spin chains [3–6]. Second, electronic charge transport through junctions of three quantum wires is governed by a variety of nontrivial fixed points which cannot be realized in two-terminal setups [7–16]. As spin currents in antiferromagnets can be induced by spin pumping [17] or by the longitudinal spin Seebeck effect [18], it is both an experimentally relevant and fundamental question to determine nontrivial fixed points governing spin transport in junctions of multiple spin chains. In particular, we are interested in the possibility of realizing a circulator for spin currents. While circulators have been discussed for photons [19–21] and for quantum Hall edge states [22,23], we are not aware of existing proposals for spin circulators. Once realized, a spin circulator has immediate applications in the field of spintronics [24], which has recently turned to the study of charge-insulating antiferromagnetic materials [25–27].

In this Rapid Communication, we study Y junctions of spin-1/2 Heisenberg chains coupled at their ends by spin-rotation [SU(2)] invariant interactions. We assume identical chains such that the junction is $\mathbb{Z}_3$ symmetric under a cyclic exchange. These conditions are respected by a chiral three-spin coupling J_χ [see Eq. (1) below], which breaks time-reversal ($\mathcal{T}$) symmetry and can be tuned from weak to strong coupling, e.g., by changing an Aharonov-Bohm flux [28–30]. Apart from condensed matter systems, such Y junctions can also be studied in ultracold atom platforms [31], where Heisenberg chains [32–34] and multispin exchange processes [35] have recently been realized. We use three complementary theoretical approaches, namely, bosonization [1], boundary conformal field theory (BCFT) [36–40], and density matrix renormalization group (DMRG) simulations [41,42].

Before entering a detailed discussion, we briefly describe our main conclusions [see Fig. 1(a)]: (i) We find two stable fixed points with emergent $\mathcal{T}$ symmetry. For small $|J_\chi|$, the renormalization group (RG) flow is towards the fixed point of open boundary conditions (O) representing disconnected chains. For large $|J_\chi|$, however, the system flows towards a spin-chain version of the three-channel Kondo fixed point [38], referred to as the K point in what follows. So far only the two-channel Kondo effect with spin chains has been studied [2,40,43]. (ii) Both stable points are separated by an unstable chiral fixed point at intermediate coupling $|J_\chi| = J_\chi^c$, where the circulation sense is determined by the sign of J_χ. DMRG simulations give $J_\chi^c/J = 3.11(1)$, where $J > 0$ is the bulk exchange coupling. (iii) Although the chiral point is unstable, it determines the physics over a wide regime of intermediate values of J_χ. It then realizes an ideal spin circulator, where incoming spin currents are scattered in a chiral (left- or right-handed) manner around the Y junction. (iv) These findings provide a key step towards realizing a chiral spin liquid (CSL), an exotic phase of frustrated quantum magnets [28,44–51]. Our spin circulator provides a building block for network constructions of CSLs [cf. Fig. 1(b)], where the chirality of each Y junction can be individually addressed.

Model. We employ the Hamiltonian $H = H_0 + H_c$, where $H_0 = \sum_{j,\alpha}(J\mathbf{S}_{j,\alpha}\cdot\mathbf{S}_{j+1,\alpha} + J_2\mathbf{S}_{j,\alpha}\cdot\mathbf{S}_{j+2,\alpha})$ describes three ($\alpha = 1,2,3$) identical semi-infinite Heisenberg chains (lattice sites $j = 1,2,\ldots$). In numerical studies, it is convenient to tune the next-nearest-neighbor coupling $J_2 = 0.2412J$ to suppress logarithmic corrections present for $J_2 = 0$ [2]. The part H_c captures couplings between the boundary spin-1/2 operators $\mathbf{S}_\alpha \equiv \mathbf{S}_{j=1,\alpha}$. We require H_c to preserve spin-SU(2) invariance and $\mathbb{Z}_3$ symmetry under a cyclic chain exchange, $\alpha \to \alpha + 1$ with $\mathbf{S}_{\alpha=4} = \mathbf{S}_1$. These conditions allow for a $\mathcal{T}$-breaking

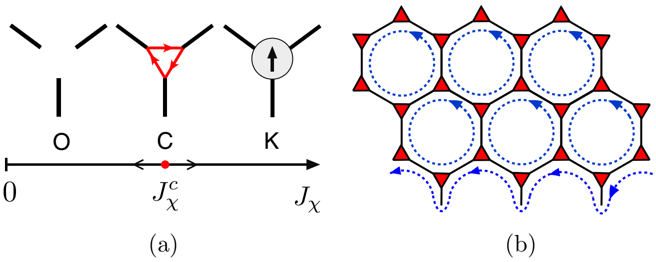

FIG. 1. Y junction and network. (a) Schematic illustration of the phase diagram. For $J_\chi < J_\chi^c$, the system flows to open boundary conditions (O fixed point), while for $J_\chi > J_\chi^c$, the three-channel Kondo (K) point is approached. The two stable fixed points are separated by an unstable chiral (C) fixed point at $J_\chi = J_\chi^c$. (b) A network of Y junctions with uniform J_χ tuned to the C point realizes a chiral spin liquid.

three-spin coupling J_χ,

$$H_c = J_\chi \hat{C}, \quad \hat{C} = \mathbf{S}_1 \cdot (\mathbf{S}_2 \times \mathbf{S}_3), \tag{1}$$

where $\hat{C}$ is the scalar spin chirality of the boundary spins [28]. We note that J_χ breaks reflection ($\mathcal{P}$) symmetry, defined as an exchange of chains 1 and 2, but H is invariant under the composite $\mathcal{PT}$ symmetry. The J_χ interaction could be realized as an effective Floquet spin model for Mott insulators pumped by circularly polarized light [30]. In principle, the ratio J_χ/J can be made arbitrarily large by varying bulk and boundary parameters independently. The above symmetries also allow for a $\mathcal{T}$-invariant boundary exchange coupling term, $J' \sum_\alpha \mathbf{S}_\alpha \cdot \mathbf{S}_{\alpha+1}$. However, since J' does not qualitatively change our conclusions, we set $J' = 0$ below [52].

Weak coupling. Let us start with the weak-coupling limit, $|J_\chi| \ll J$. In the low-energy continuum limit and for decoupled chains, spin operators take the form ($x = ja$ with lattice constant a) [1]

$$\mathbf{S}_\alpha(x) = \mathbf{J}_{L,\alpha}(x) + \mathbf{J}_{R,\alpha}(x) + (-1)^j \mathbf{n}_\alpha(x), \tag{2}$$

where chiral spin currents $\mathbf{J}_{L/R,\alpha}(x)$ represent the smooth part and $\mathbf{n}_\alpha(x)$ the staggered magnetization. Using Abelian bosonization, we express these operators in terms of chiral bosons $\varphi_{L/R,\alpha}(x)$ or, equivalently, dual fields $\phi_\alpha(x) = (\varphi_{L,\alpha} - \varphi_{R,\alpha})/\sqrt{2}$ and $\theta_\alpha(x) = (\varphi_{L,\alpha} + \varphi_{R,\alpha})/\sqrt{2}$ [1]. With the nonuniversal constant $A \sim 1/a$ and $\nu = L/R = +/-$, one finds

$$J^z_{\nu,\alpha}(x) = \frac{\nu}{\sqrt{4\pi}} \partial_x \varphi_{\nu,\alpha}, \quad J^\pm_{\nu,\alpha}(x) = \frac{1}{2\pi a} e^{\pm i\sqrt{4\pi}\varphi_{\nu,\alpha}},$$
$$n^z_\alpha(x) = A \sin[\sqrt{2\pi}\phi_\alpha], \quad n^\pm_\alpha(x) = A e^{\pm i\sqrt{2\pi}\theta_\alpha}. \tag{3}$$

For $J_\chi = 0$, open boundary conditions at $x = 0$ are imposed by writing $\varphi_{R,\alpha}(x) = \varphi_{L,\alpha}(-x) + \varphi_0$ [1], where SU(2) invariance requires $\varphi_0 = 0$ or $\varphi_0 = \sqrt{\pi}$. In terms of SU(2) currents, we have $\mathbf{J}_{R,\alpha}(x) = \mathbf{J}_{L,\alpha}(-x)$. The effective low-energy Hamiltonian can be written as $H_0 \simeq (2\pi v/3) \sum_\alpha \int_{-\infty}^{+\infty} dx\, \mathbf{J}^2_{L,\alpha}$, where $v \approx 1.17Ja$ [2] is the spin velocity for $J_2 = 0.2412J$. This model has a central charge $c = 3$ corresponding to three decoupled $SU(2)_1$ Wess-Zumino-Novikov-Witten (WZNW) models [1,53]. We can then analyze the perturbations to the O point that arise for $|J_\chi| \ll J$. Boundary spin operators follow from Eq. (2) as $\mathbf{S}_\alpha \propto \mathbf{J}_{L,\alpha}(0)$ [2]. The three-spin interaction $\sim J_\chi \mathbf{J}_{L,1}(0) \cdot [\mathbf{J}_{L,2}(0) \times \mathbf{J}_{L,3}(0)]$ has scaling dimension three and is irrelevant. In fact, it is more irrelevant than the leading $\mathcal{T}$-invariant perturbation $\sum_\alpha \mathbf{J}_{L,\alpha}(0) \cdot \mathbf{J}_{L,\alpha+1}(0)$ (dimension two), which is generated by the RG to second order in J_χ.

Strong coupling. Next, we address the limit $|J_\chi| \gg J$. For $J = 0$, one can readily diagonalize the three-spin Hamiltonian H_c [28]. The ground state of H_c is twofold degenerate and, assuming $J_\chi > 0$, has an eigenvalue $-\sqrt{3}/4$ of $\hat{C}$. In the $|S_1^z, S_2^z, S_3^z\rangle$ boundary spin basis, the ground state with eigenvalue $M = +1/2$ of $\sum_\alpha S^z_\alpha$ is given by

$$|+\rangle = \frac{i}{\sqrt{3}}(|\downarrow\uparrow\uparrow\rangle + \omega|\uparrow\uparrow\downarrow\rangle + \omega^2|\uparrow\downarrow\uparrow\rangle), \quad \omega = e^{2\pi i/3}. \tag{4}$$

The $|-\rangle$ state with $M = -1/2$ follows by $\mathcal{PT}$ conjugation. All other states involve an energy cost of order J_χ. For finite $J \ll J_\chi$, the low-energy physics therefore involves an effective spin-1/2 operator $\mathbf{S}_{\rm imp}$ acting in the $\{|+\rangle, |-\rangle\}$ subspace. By projecting H onto this subspace, we arrive at a spin-chain version of the three-channel Kondo model,

$$\tilde{H} = H_0 + J_K \mathbf{S}_{\rm imp} \cdot \sum_\alpha [\mathbf{S}_{2,\alpha} + (J_2/J)\mathbf{S}_{3,\alpha}], \tag{5}$$

where $J_K \simeq J/3$. Since $\mathbf{S}_{\rm imp}$ is built from the original boundary spins $\mathbf{S}_{j=1,\alpha}$, the latter disappear from H_0 and the boundary is now at site $j = 2$. The exchange coupling J_K is marginally relevant. As a consequence, Kondo screening processes drive the system towards a strong-coupling fixed point identified with the K point. The physics of the K point is realized at energy scales below the Kondo temperature $T_K \sim J e^{-1/\lambda_0}$, where $\lambda_0 \approx J_K a/(2\pi v)$ [54]. Although the projected Hamiltonian in Eq. (5) lacks $\mathcal{T}$-breaking interactions, such interactions are generated by a Schrieffer-Wolff transformation to first order in J/J_χ. However, they turn out to be irrelevant [52]. Before analyzing the K point using BCFT, we turn to the critical point separating the stable O and K points.

Chiral fixed point. We define the chirality $\hat{C}_j = \mathbf{S}_{j,1} \cdot (\mathbf{S}_{j,2} \times \mathbf{S}_{j,3})$ for three spins at site j in different chains [cf. Eq. (1)]. In the continuum limit, the most relevant contribution to $\hat{C}_j$ stems from the staggered magnetization, $\hat{C}_j \sim \mathbf{n}_1(x) \cdot [\mathbf{n}_2(x) \times \mathbf{n}_3(x)]$. Energetic considerations suggest that $J_\chi \neq 0$ should favor a fixed point in which $\hat{C} = \hat{C}_1$ acquires a nonzero expectation value. This happens if we impose

$$\varphi_{R,\alpha\pm 1}(x) = \varphi_{L,\alpha}(-x) + \varphi_0. \tag{6}$$

As for the O point, SU(2) invariance requires $\varphi_0 = 0$ or $\varphi_0 = \sqrt{\pi}$. Equation (6) implements ideal chiral boundary conditions for the spin currents,

$$\mathbf{J}_{R,\alpha\pm 1}(0) = \mathbf{J}_{L,\alpha}(0). \tag{7}$$

We refer to the corresponding fixed points as $C_\pm$, respectively.

Ideal spin circulator. To see that the $C_\pm$ points realize an ideal spin circulator, we consider the linear spin conductance tensor (with arbitrary $y > 0$ and $\omega \to i0^+$) [11,55]

$$\mathbb{G}^{bb'}_{\alpha\alpha'} = -\frac{(g\mu_B)^2}{\hbar L \omega} \int_0^L dx \int_{-\infty}^{\infty} d\tau\, e^{i\omega\tau} \langle \mathcal{T}_\tau J^b_\alpha(x,\tau) J^{b'}_{\alpha'}(y,0) \rangle, \tag{8}$$

which determines the spin current in chain α with polarization direction $\hat{e}_{b=x,y,z}$ in response to a spin chemical potential [26,27] applied in chain α' with polarization $\hat{e}_{b'}$. Here, g denotes the gyromagnetic ratio, μ_B the Bohr magneton, L the chain length, $\mathcal{T}_\tau$ the imaginary-time (τ) ordering operator, and the spin current density is $\mathbf{J}_\alpha = \mathbf{J}_{R,\alpha} - \mathbf{J}_{L,\alpha}$ [cf. Eq. (2)]. Using the boundary conditions in Eq. (7), we obtain from Eq. (8) the maximally asymmetric tensor

$$\mathbb{G}^{bb'}_{\alpha\alpha'} = \frac{(g\mu_B)^2}{2\pi\hbar}\delta^{bb'}(\delta_{\alpha,\alpha'} - \delta_{\alpha\pm1,\alpha'}) \quad (\text{for } \mathrm{C}_\pm). \tag{9}$$

Right at the C_+ or C_- point, an incoming spin current is therefore completely channeled into the adjacent chain $\alpha \pm 1$ (cf. Fig. 1), without polarization change. The Y junction then represents an ideal spin circulator.

Realizing the chiral point. It remains to show that the $\mathrm{C}_\pm$ points can be realized at intermediate J_χ. We first approach the problem from the weak-coupling side. Despite being energetically favored by $J_\chi \neq 0$, the $\mathrm{C}_\pm$ points must be unstable since the O point is stable for $|J_\chi| \ll J$. Indeed, a relevant boundary perturbation H_1 is generated by the three-spin coupling when using Eq. (2) and imposing either of the conditions (6),

$$H_1 = \lambda_1 \sum_\alpha \cos\{\sqrt{\pi}[\varphi_{L,\alpha}(0) - \varphi_{L,\alpha+1}(0)]\}. \tag{10}$$

Using bosonization, we find $\lambda_1 < 0$ and $|\lambda_1| \propto |J_\chi|$ for $|J_\chi| \ll J$. The physical process behind this dimension-1/2 operator is the backscattering of spin currents [11]. For $\lambda_1 < 0$, the RG flow approaches $\lambda_1 \to -\infty$ at low energies. Pinning the boson fields to the respective cosine minima in Eq. (10) takes the system back to the O point. Since at weak coupling there is only one relevant perturbation allowed by $\mathbb{Z}_3$ symmetry, the C point can be reached by fine tuning a single parameter λ_1, e.g., by increasing J_χ. Let us assume that there is a critical value J_χ^c such that $\lambda_1(J_\chi^c) = 0$. For $J_\chi > 0$ ($J_\chi < 0$), this putative critical point corresponds to the C_- (C_+) point.

Now consider approaching the C point from the strong-coupling side. For $J_\chi > J_\chi^c$, the relevant coupling constant becomes positive, $\lambda_1 > 0$, and the RG flow approaches $\lambda_1 \to +\infty$. The pinning conditions now involve a π-phase shift for the cosine terms in Eq. (10) as compared to $J_\chi < J_\chi^c$. For the total magnetization $S^z_{\rm tot} = -\sum_\alpha[\varphi_{L,\alpha}(0) - \varphi_{R,\alpha}(0)]/\sqrt{2\pi}$, this shift means that an effective spin-1/2 degree of freedom has been brought from infinity to the boundary. This is precisely what we expect from the formation of the impurity spin in the strong-coupling regime. The coupling of the impurity spin to the bulk allows for a second dimension-1/2 boundary operator, $H_2 = \lambda_2 \mathbf{S}_{\rm imp} \cdot \sum_\alpha \tilde{\mathbf{n}}_\alpha(0)$, where $\tilde{\mathbf{n}}_\alpha$ is the staggered magnetization after imposing Eq. (6). The flow of λ_1 and λ_2 to strong coupling leads to a fixed point where the impurity spin is overscreened by the three chains, which we identify with the K point.

Since λ_1 vanishes at the critical point, the effects of the dimension-1/2 perturbations are felt only when the renormalized couplings at energy scale $\mathcal{E}$ become of order one. We thus obtain a wide quantum critical regime, $(1 - J_\chi/J_\chi^c)^2 \lesssim \mathcal{E}/J \ll 1$, where the physics is governed by the C point. Related but different chiral points have been discussed for electronic Y junctions [11]. The latter are stable for attractive electron-electron interactions and the asymmetry of the charge conductance tensor depends on the interaction strength. By

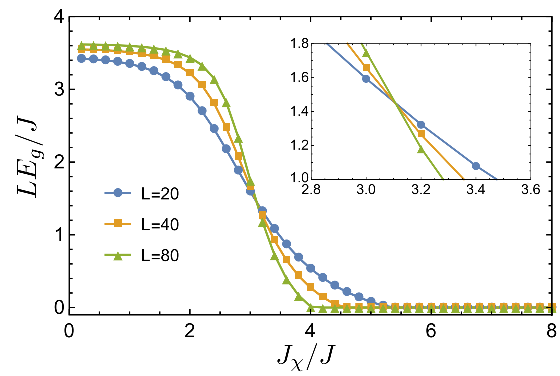

FIG. 2. DMRG results for the finite-size energy gap E_g, rescaled by the chain length L, vs J_χ/J for several L. The inset highlights the crossing that determines the critical point.

contrast, our C point is unstable, but due to SU(2) symmetry the spin conductance (9) is universal and maximally asymmetric.

BCFT approach. A spin-1/2 impurity coupled with equal strength to the open ends of two spin chains realizes a spin version of the two-channel Kondo effect [2,40,43]. Here, we develop a BCFT approach and extend this analogy to three channels. We employ the conformal embedding $\mathrm{SU}(2)_3 \times \mathbb{Z}_3^{(5)}$, whereby the total central charge $c = 3$ is split into a $\mathrm{SU}(2)_3$ WZNW model (with $c = 9/5$), representing the spin degree of freedom, and a parafermionic $\mathbb{Z}_3^{(5)}$ CFT (with $c = 6/5$) [56–60], representing the "flavor" (i.e., channel) degree of freedom.

The RG fixed points are characterized by conformally invariant boundary conditions [36–38]. The spectrum of the theory is encoded by the partition function $Z_{\rm AB}$ on the cylinder with boundary conditions A and B. For instance, $Z_{\rm OO}$ represents the partition function with open boundary conditions at both ends. Partition functions with other boundary conditions can be generated via fusion [37]. The boundary operators that perturb the K point can be determined using double fusion with the spin-1/2 primary in the $\mathrm{SU}(2)_3$ sector [39,40]. The leading irrelevant operator is the Kac-Moody descendant $\boldsymbol{\mathcal{J}}_{-1} \cdot \boldsymbol{\phi}_1$, where $\boldsymbol{\mathcal{J}}$ is the $\mathrm{SU}(2)_3$ current and $\boldsymbol{\phi}_1$ is the spin-1 primary. This $\mathcal{T}$-invariant operator has scaling dimension $\Delta = 7/5$, as in the free-electron three-channel Kondo model [38,39]. Similarly, the leading chiral boundary operator at the K point is the dimension-8/5 field of $\mathbb{Z}_3^{(5)}$ [57]. Moreover, the effective Hamiltonian at the K point includes only irrelevant boundary operators in the presence of cyclic exchange symmetry [52].

DMRG results. We now describe numerical results for Y junctions with chain length L using the DMRG algorithm by Guo and White [61], which works efficiently for open boundary conditions at $j = L$. First, we look for the critical point by analyzing the finite-size gap E_g between the lowest-energy state with $S^z_{\rm tot} = \sum_{j,\alpha} S^z_{j,\alpha} = 0$ and the one with $S^z_{\rm tot} = 1$. For large L, at weak coupling we expect E_g to approach the singlet-triplet gap of decoupled chains (O point), $E_g = \pi v/L$. On the other hand, at strong coupling, the BCFT approach predicts (through the partition function $Z_{\rm KO}$ [52]) that the ground state is a triplet and hence E_g should vanish identically. We indeed observe a (L-dependent) level crossing between a singlet ground state for small J_χ and a triplet for large J_χ

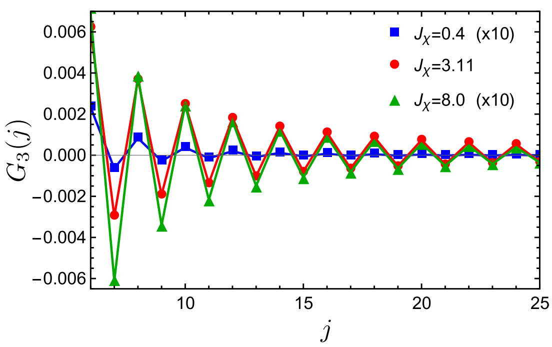

FIG. 3. Three-spin correlations $G_3(j)$ vs distance from the junction for $L = 80$ and three values of J_χ. The data for $J_\chi = 0.4\,J$ and $J_\chi = 8\,J$ are scaled up by a factor 10. Solid lines represent fits to a power-law decay.

(see Fig. 2). The critical point is then determined from the crossing of the LE_g vs J_χ curves for $40 \leqslant L \leqslant 80$, resulting in $J_\chi^c/J = 3.11(1)$.

Next, we calculate the three-spin ground-state correlation function $G_3(j) = \langle \hat{C}_j \rangle = \langle \mathbf{S}_{j,1} \cdot (\mathbf{S}_{j,2} \times \mathbf{S}_{j,3}) \rangle$. At the C point, the long-distance decay of $G_3(j)$ is governed by the bulk scaling dimension of $\hat{C}_j$, where our BCFT predicts $G_3(j) \sim (-1)^j j^{-\nu_C}$ with $\nu_C = 3/2$. Near the $\mathcal{T}$-symmetric O and K points, the leading chiral boundary operator has dimension $\Delta_O = 3$ and $\Delta_K = 8/5$, respectively. Standard perturbation theory around these fixed points yields $G_3(j) \sim (-1)^j j^{-\nu_{O,K}}$ with $\nu_O = 7/2$ and $\nu_K = 21/10$, respectively. Our DMRG results for $G_3(j)$ are shown in Fig. 3. First, we note that $G_3(j)$ has a much larger magnitude and decays more slowly at the critical point. Fitting the numerical results to a power-law expression with smooth and staggered parts yields the exponent $\nu(J_\chi)$ of the dominant staggered term as listed in Table I. For the fit, we only took into account data for $G_3(j)$ with $8 \leqslant j \leqslant L/2$ in order to avoid both the nonuniversal short-distance behavior and effects due to the open boundary at $j = L$. [Results for $\nu(J_\chi)$ are robust under changes of the fitting interval [52].] Our DMRG results in Table I agree well with the analytical predictions. The deviation is most significant at the C point, where one, however, also observes the strongest finite-size effects. We emphasize that the DMRG results show a slow decay of $G_3(j)$ over a wide region around the critical point.

TABLE I. Exponent $\nu(J_\chi)$ obtained by fitting the decay of $G_3(j)$ in the interval $8 \leqslant j \leqslant L/2$. The extrapolated value follows from a second-order polynomial fit. The last column shows the predictions for the O, C, and K points, respectively.

J_χ/J	$L = 40$	$L = 60$	$L = 80$	Extrap.	Expected
0.4	3.56	3.51	3.49	3.45	3.5
3.11	1.89	1.79	1.74	1.59	1.5
8	2.31	2.22	2.18	2.08	2.1

Conclusions and outlook. We have demonstrated that a Y junction of the Heisenberg chains acts as a quantum spin circulator in the vicinity of a critical point reached by tuning the three-spin interaction J_χ. In addition to applications as a nonreciprocal device for pure spin transport, this spin circulator can be used for constructing two-dimensional networks realizing CSL phases, where the chirality of each node can be independently tuned [30]. In fact, such an approach could allow for the systematic design of synthetic quantum materials harboring CSL phases. For instance, the network with uniform chirality shown in Fig. 1(b) has spin modes circulating in closed loops in the bulk. The bulk quasiparticles can be defined from the spin-1/2 field of the chiral WZNW model in each loop [49] and have a finite gap due to the finite length of the loops. In addition, there is a gapless chiral edge mode with quantized spin conductance, cf. Fig. 1(b). This corresponds to the properties of the Kalmeyer-Laughlin CSL, a topological phase equivalent to a bosonic fractional quantum Hall system [44,46]. Furthermore, one can consider networks with alternating sign of J_χ, i.e., staggered chirality between the nodes. This may shed light on the much less understood gapless CSLs with spinon Fermi surfaces [45,50].

Acknowledgments. We thank I. Affleck, E. Ercolessi, F. Ravanini, A. Tsvelik, and J. C. Xavier for discussions. We acknowledge funding by the Deutsche Forschungsgemeinschaft within the network CRC TR 183 (Project No. C01) and by CNPq (R.G.P.).

[1] A. Gogolin, A. Nersesyan, and A. Tsvelik, *Bosonization and Strongly Correlated Systems* (Cambridge University Press, 2004).
[2] S. Eggert and I. Affleck, Phys. Rev. B **46**, 10866 (1992).
[3] A. M. Tsvelik, Phys. Rev. Lett. **110**, 147202 (2013).
[4] N. Crampé and A. Trombettoni, Nucl. Phys. B **871**, 526 (2013).
[5] A. M. Tsvelik and W.-G. Yin, Phys. Rev. B **88**, 144401 (2013).
[6] F. Buccheri, H. Babujian, V. E. Korepin, P. Sodano, and A. Trombettoni, Nucl. Phys. B **896**, 52 (2015).
[7] C. Nayak, M. P. A. Fisher, A. W. W. Ludwig, and H. H. Lin, Phys. Rev. B **59**, 15694 (1999).
[8] S. Chen, B. Trauzettel, and R. Egger, Phys. Rev. Lett. **89**, 226404 (2002).
[9] C. Chamon, M. Oshikawa, and I. Affleck, Phys. Rev. Lett. **91**, 206403 (2003).
[10] X. Barnabé-Thériault, A. Sedeki, V. Meden, and K. Schönhammer, Phys. Rev. Lett. **94**, 136405 (2005).
[11] M. Oshikawa, C. Chamon, and I. Affleck, J. Stat. Mech.: Theory Exp. (2006) P02008.
[12] C.-Y. Hou and C. Chamon, Phys. Rev. B **77**, 155422 (2008).
[13] D. Giuliano and P. Sodano, Nucl. Phys. B **811**, 395 (2009).
[14] A. Agarwal, S. Das, S. Rao, and D. Sen, Phys. Rev. Lett. **103**, 026401 (2009).
[15] B. Bellazzini, M. Mintchev, and P. Sorba, Phys. Rev. B **80**, 245441 (2009).
[16] A. Rahmani, C.-Y. Hou, A. Feiguin, M. Oshikawa, C. Chamon, and I. Affleck, Phys. Rev. B **85**, 045120 (2012).
[17] R. Cheng, J. Xiao, Q. Niu, and A. Brataas, Phys. Rev. Lett. **113**, 057601 (2014).

[18] D. Hirobe, M. Sato, T. Kawamata, Y. Shiomi, K.-i. Uchida, R. Iguchi, Y. Koike, S. Maekawa, and E. Saitoh, Nat. Phys. **13**, 30 (2016).
[19] M. Scheucher, A. Hilico, E. Will, J. Volz, and A. Rauschenbeutel, Science **354**, 1577 (2016).
[20] P. Lodahl, S. Mahmoodian, S. Stobbe, A. Rauschenbeutel, P. Schneeweiss, J. Volz, H. Pichler, and P. Zoller, Nature (London) **541**, 473 (2017).
[21] B. J. Chapman, E. I. Rosenthal, J. Kerckhoff, B. A. Moores, L. R. Vale, J. A. B. Mates, G. C. Hilton, K. Lalumière, A. Blais, and K. W. Lehnert, Phys. Rev. X **7**, 041043 (2017).
[22] G. Viola and D. P. DiVincenzo, Phys. Rev. X **4**, 021019 (2014).
[23] A. C. Mahoney, J. I. Colless, S. J. Pauka, J. M. Hornibrook, J. D. Watson, G. C. Gardner, M. J. Manfra, A. C. Doherty, and D. J. Reilly, Phys. Rev. X **7**, 011007 (2017).
[24] S. A. Wolf, D. D. Awschalom, R. A. Buhrman, J. M. Daughton, S. von Molnár, M. L. Roukes, A. Y. Chtchelkanova, and D. M. Treger, Science **294**, 1488 (2001).
[25] P. Wadley, B. Howells, J. Železný, C. Andrews, V. Hills, R. P. Campion, V. Novák, K. Olejník, F. Maccherozzi, S. S. Dhesi, S. Y. Martin, T. Wagner, J. Wunderlich, F. Freimuth, Y. Mokrousov, J. Kuneš, J. S. Chauhan, M. J. Grzybowski, A. W. Rushforth, K. W. Edmonds, B. L. Gallagher, and T. Jungwirth, Science **351**, 587 (2016).
[26] T. Jungwirth, X. Marti, P. Wadley, and J. Wunderlich, Nat. Nanotechnol. **11**, 231 (2016).
[27] V. Baltz, A. Manchon, M. Tsoi, T. Moriyama, T. Ono, and Y. Tserkovnyak, Rev. Mod. Phys. **90**, 015005 (2018).
[28] X. G. Wen, F. Wilczek, and A. Zee, Phys. Rev. B **39**, 11413 (1989).
[29] D. Sen and R. Chitra, Phys. Rev. B **51**, 1922 (1995).
[30] M. Claassen, H.-C. Jiang, B. Moritz, and T. P. Devereaux, Nat. Commun. **8**, 1192 (2017).
[31] T. Esslinger, Annu. Rev. Condens. Matter Phys. **1**, 129 (2010).
[32] S. Murmann, F. Deuretzbacher, G. Zürn, J. Bjerlin, S. M. Reimann, L. Santos, T. Lompe, and S. Jochim, Phys. Rev. Lett. **115**, 215301 (2015).
[33] M. Boll, T. A. Hilker, G. Salomon, A. Omran, J. Nespolo, L. Pollet, I. Bloch, and C. Gross, Science **353**, 1257 (2016).
[34] M. Endres, H. Bernien, A. Keesling, H. Levine, E. R. Anschuetz, A. Krajenbrink, C. Senko, V. Vuletic, M. Greiner, and M. D. Lukin, Science **354**, 1024 (2016).
[35] H.-N. Dai, B. Yang, A. Reingruber, H. Sun, X.-F. Xu, Y.-A. Chen, Z.-S. Yuan, and J.-W. Pan, Nat. Phys. **13**, 1195 (2017).
[36] J. L. Cardy, Nucl. Phys. B **275**, 200 (1986).
[37] J. L. Cardy, Nucl. Phys. B **324**, 581 (1989).
[38] I. Affleck and A. W. W. Ludwig, Nucl. Phys. B **352**, 849 (1991).
[39] I. Affleck and A. W. W. Ludwig, Nucl. Phys. B **360**, 641 (1991).
[40] I. Affleck, arXiv:cond-mat/9311054.
[41] S. R. White, Phys. Rev. Lett. **69**, 2863 (1992).
[42] U. Schollwöck, Rev. Mod. Phys. **77**, 259 (2005).
[43] B. Alkurtass, A. Bayat, I. Affleck, S. Bose, H. Johannesson, P. Sodano, E. S. Sørensen, and K. Le Hur, Phys. Rev. B **93**, 081106 (2016).
[44] V. Kalmeyer and R. B. Laughlin, Phys. Rev. Lett. **59**, 2095 (1987).
[45] B. Bauer, B. P. Keller, M. Dolfi, S. Trebst, and A. W. W. Ludwig, arXiv:1303.6963.
[46] B. Bauer, L. Cincio, B. P. Keller, M. Dolfi, G. Vidal, S. Trebst, and A. W. W. Ludwig, Nat. Commun. **5**, 5137 (2014).
[47] Y.-C. He, D. N. Sheng, and Y. Chen, Phys. Rev. Lett. **112**, 137202 (2014).
[48] S.-S. Gong, W. Zhu, and D. N. Sheng, Sci. Rep. **4**, 6317 (2014).
[49] G. Gorohovsky, R. G. Pereira, and E. Sela, Phys. Rev. B **91**, 245139 (2015).
[50] S. Bieri, L. Messio, B. Bernu, and C. Lhuillier, Phys. Rev. B **92**, 060407 (2015).
[51] K. Kumar, H. J. Changlani, B. K. Clark, and E. Fradkin, Phys. Rev. B **94**, 134410 (2016).
[52] See Supplemental Material at http://link.aps.org/supplemental/10.1103/PhysRevB.97.220402, where we specify the full low-energy theory in the strong-coupling limit and provide additional details about the BCFT approach and DMRG methods.
[53] I. Affleck and F. D. M. Haldane, Phys. Rev. B **36**, 5291 (1987).
[54] N. Laflorencie, E. S. Sørensen, and I. Affleck, J. Stat. Mech.: Theory Exp. (2008) P02007.
[55] F. Meier and D. Loss, Phys. Rev. Lett. **90**, 167204 (2003).
[56] A. Zamolodchikov and V. Fateev, JETP **62**, 215 (1985).
[57] V. Fateev and A. Zamolodchikov, Nucl. Phys. B **280**, 644 (1987).
[58] E. Frenkel, V. Kac, and M. Wakimoto, Commun. Math. Phys. **147**, 295 (1992).
[59] K. Totsuka and M. Suzuki, J. Phys. A: Math. Gen. **29**, 3559 (1996).
[60] I. Affleck, M. Oshikawa, and H. Saleur, Nucl. Phys. B **594**, 535 (2001).
[61] H. Guo and S. R. White, Phys. Rev. B **74**, 060401 (2006).